

Complete Characterization of Quantum Correlations by Randomized Measurements

Nikolai Wyderka¹, Andreas Ketterer², Satoya Imai³, Jan Lennart Bönsel³, Daniel E. Jones⁴,
 Brian T. Kirby^{4,5}, Xiao-Dong Yu³, and Otfried Gühne³


¹*Institut für Theoretische Physik III, Heinrich-Heine-Universität Düsseldorf, Universitätsstr. 1, 40225 Düsseldorf, Germany*

²*Fraunhofer Institute for Applied Solid State Physics IAF, Tullastr. 72, 79108 Freiburg, Germany*

³*Naturwissenschaftlich-Technische Fakultät, Universität Siegen, Walter-Flex-Str. 3, 57068 Siegen, Germany*

⁴*DEVCOM Army Research Laboratory, Adelphi, Maryland 20783, USA*

⁵*Tulane University, New Orleans, Louisiana 70118, USA*

 (Received 28 February 2023; revised 15 June 2023; accepted 10 August 2023; published 28 August 2023)

The fact that quantum mechanics predicts stronger correlations than classical physics is an essential cornerstone of quantum information processing. Indeed, these quantum correlations are a valuable resource for various tasks, such as quantum key distribution or quantum teleportation, but characterizing these correlations in an experimental setting is a formidable task, especially in scenarios where no shared reference frames are available. By definition, quantum correlations are reference-frame independent, i.e., invariant under local transformations; this physically motivated invariance implies, however, a dedicated mathematical structure and, therefore, constitutes a roadblock for an efficient analysis of these correlations in experiments. Here we provide a method to directly measure any locally invariant property of quantum states using locally randomized measurements, and we present a detailed toolbox to analyze these correlations for two quantum bits. We implement these methods experimentally using pairs of entangled photons, characterizing their usefulness for quantum teleportation and their potential to display quantum nonlocality in its simplest form. Our results can be applied to various quantum computing platforms, allowing simple analysis of correlations between arbitrary distant qubits in the architecture.

DOI: [10.1103/PhysRevLett.131.090201](https://doi.org/10.1103/PhysRevLett.131.090201)

Introduction.—Quantum mechanics contains a plethora of fascinating nonlocal effects that are useful in various applications of quantum technologies. Such effects are, by definition, invariant under changes of the local reference systems or, mathematically speaking, of the choice of the local bases of the Hilbert space. This naturally leads to the expectation that they should be describable by quantities which are invariant under such transformations. A quantum state of composite systems is described by a density matrix ρ_{AB} in the tensor product space of the individual systems, so invariance under local basis changes of any function $f(\rho_{AB})$ of the state can, in the case of bipartite systems, be expressed as

$$f(\rho_{AB}) = f(U_A \otimes U_B \rho_{AB} U_A^\dagger \otimes U_B^\dagger), \quad (1)$$

where U_A and U_B are unitary matrices governing the basis change of the first and second system, respectively. Because of this invariance, an average over all such transformations yields

$$f(\rho_{AB}) = \iint dU_A dU_B f(U_A \otimes U_B \rho_{AB} U_A^\dagger \otimes U_B^\dagger). \quad (2)$$

On the other hand, any physical function may be expanded in terms of powers of expectation values of certain observables, yielding

$$f(\rho_{AB}) = \sum_{\vec{t}} c_{\vec{t}} \langle \mathcal{M}_1 \rangle^{t_1} \langle \mathcal{M}_2 \rangle^{t_2} \dots \quad (3)$$

for appropriately chosen bipartite observables \mathcal{M}_i and coefficients $c_{\vec{t}}$, where $\vec{t} = (t_1, t_2, \dots)$ denotes all possible multi-indices with positive integers t_i and a varying number of entries k . Combining this with local unitary invariance yields

$$f(\rho_{AB}) = \sum_{\vec{t}} c_{\vec{t}} \mathcal{R}_{\mathcal{M}_1}^{(t_1)}(\rho_{AB}) \mathcal{R}_{\mathcal{M}_2}^{(t_2)}(\rho_{AB}) \dots, \quad (4)$$

where the quantities

$$\mathcal{R}_{\mathcal{M}}^{(t)}(\rho) := \iint dU_A dU_B \{ \text{Tr}[(U_A \otimes U_B) \rho (U_A^\dagger \otimes U_B^\dagger) \mathcal{M}] \}^t \quad (5)$$

are the t th moments of the probability distribution of measurement results for the bipartite observable \mathcal{M} under random local basis changes. For the case of product observables, the quantities $\mathcal{R}_{A \otimes B}^{(t)}$ have been studied as randomized measurements, see, e.g., Refs. [1–5]. The advantages of these schemes include the possibility to obtain the data without having shared reference frames,

having limited control over the measurements and in the presence of uncharacterized local unitary noise. With sufficient experimental control, the random unitaries may even be selected from a finite unitary t design instead [6,7]. Note that the mild assumptions on the measurement capabilities are in contrast to the stronger ones in shadow tomography schemes, where known random unitary rotations are applied to a state to estimate expectation values with a small number of measurements [8].

Here, we go beyond the standard randomized measurement schemes by allowing for non-product observables. While this sounds like a disadvantage for practical implementations, we stress that it is possible to obtain the moment data for nonproduct observables from the data of multiple product observables by classical postprocessing.

As the moments of these distributions can be measured directly, they form the main objects of interest in order to describe the local unitary invariant functions. In principle, it is possible to expand any (polynomial) local unitary invariant (LU invariant) in this manner. However, so far only a small subset of these moments has been exploited for tasks like entanglement detection [9–12] or fidelity estimation [13,14].

In this Letter, we develop a general framework linking the moments of randomized measurements and the set of LU invariants. For fixed local dimension d , the set of polynomial invariants is finitely generated [15,16], so it suffices to consider the generators. Indeed, complete sets of generators have been found in the case of two-qubit states and certain classes of higher-dimensional cases [17,18]. In the following, we develop concrete schemes to measure *all* of the relevant two-qubit invariants, but naturally our theory can be extended to known invariants in higher-dimensional or multiparticle systems. We illustrate this by deriving a scheme to measure the Kempe invariant in three-qubit systems [19,20]. As an application, we experimentally implement a randomized measurement scheme to measure some of the invariants and use it to certify the presence of Bell nonlocality and the usefulness of the prepared states for teleportation schemes.

Randomized measurements.—In the framework of randomized measurements, a multiparticle quantum state undergoes random local unitary transformations before a fixed observable \mathcal{M} is measured. The experiment is repeated a number of times for different choices of local unitaries. From the statistics and the moments of the resulting probability distribution, one then aims to infer properties of the underlying quantum state.

More formally, the quantities obtained in the experiment for a bipartite quantum state ρ are those given in Eq. (5), where the integrals are evaluated with respect to the Haar measure over the unitary group $\mathcal{U}(d)$, the measured observable is denoted \mathcal{M} , and the moment of the corresponding probability distribution is denoted by t .

In this Letter, we are mainly concerned with two-qubit states, for which a complete generating set of 18

polynomial invariants has been characterized before [17]. Of these invariants, six are needed only to distinguish certain specific states by the signs of these invariants, thus we do not expect to extract relevant information in terms of entanglement or nonlocality from these. The remaining twelve invariants are of degree up to six. In order to express them properly, let us decompose the bipartite quantum state in terms of the Bloch representation, i.e., we write

$$\rho = \frac{1}{4} \left[\mathbb{1} \otimes \mathbb{1} + \vec{\alpha} \cdot \vec{\sigma} \otimes \mathbb{1} + \mathbb{1} \otimes \vec{\beta} \cdot \vec{\sigma} + \sum_{i,j=1}^3 T_{ij} \sigma_i \otimes \sigma_j \right], \quad (6)$$

where $\sigma_{1,2,3}$ denote the usual Pauli matrices. Thus, the state is determined by its local Bloch vectors $\vec{\alpha}$ and $\vec{\beta}$, and the real correlation matrix T . In terms of these, the invariants can be expressed conveniently, and we give a complete list in Appendix A in the Supplemental Material [21]. For our purposes, we will focus on the invariants $I_1 = \det(T)$, $I_2 = \text{Tr}(TT^T)$ and $I_3 = \text{Tr}(TT^T TT^T)$. With the help of these three invariants, it is possible to decide whether the state can violate a CHSH-like Bell inequality. Furthermore, it is possible to bound the teleportation fidelity of the state.

Two of the invariants, including I_1 , are special in the sense that they flip signs under partial transposition of ρ , whereas all other invariants do not. This has consequences on how to measure them: While the other invariants can be obtained from the statistics of product observables, I_1 and I_{14} require nonproduct observables. In turn, they are linked to the entanglement of the state and can be used to obtain the entanglement measure of negativity of the state using randomized measurements [36], see Appendix A for more details [21].

Expressions for the LU invariants.—Let us now state explicitly how to measure the LU invariants in a randomized measurement scheme. To that end, recall that in order to observe the moments in Eq. (5), one has to choose an appropriate observable. Here, we show how to choose it in order to obtain the invariants I_1 , I_2 and I_3 .

As a first example, we explore the moments in case of the choice $\mathcal{M} = Z \otimes Z$. Note that choosing any other combination of Pauli matrices yields the same results, as they are related by local unitary rotations. For this choice, the first moment vanishes and we obtain as the second moment

$$\mathcal{R}_{Z \otimes Z}^{(2)} = \frac{1}{9} \text{Tr}(TT^T) = \frac{1}{9} I_2, \quad (7)$$

where the occurring integrals can be solved using Weingarten calculus [37].

Next, $t = 3$ yields again zero (as well as any odd moment). For $t = 4$, we obtain

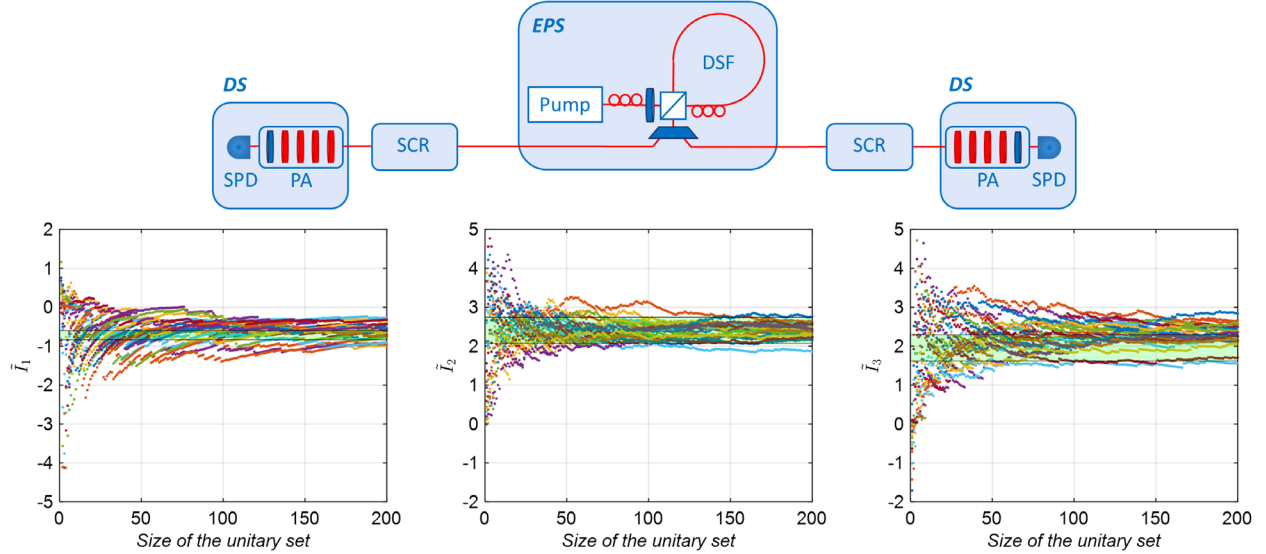


FIG. 1. (a) Schematic diagram of the experimental setup for performing the randomized measurement protocol with polarization-entangled photon pairs. Detector station (DS), dispersion-shifted fiber (DSF), entangled photon source (EPS), polarization analyzer (PA), polarization scrambler (SCR), single photon detector (SPD). (b),(c),(d) Experimentally determined unbiased estimators for the invariants I_1 , I_2 , and I_3 for 25 different runs consisting of measurements with 200 different random unitaries. The black lines show the expected values of each parameter calculated from the density matrix of the experimental system.

$$\begin{aligned} \mathcal{R}_{Z \otimes Z}^{(4)} &= \frac{1}{75} [2\text{Tr}(TT^T TT^T) + \text{Tr}(TT^T)^2] \\ &= \frac{1}{75} [2I_3 + I_2^2], \end{aligned} \quad (8)$$

giving access to the invariant I_3 .

Finally, as $I_1 = \det(T)$ flips sign under partial transposition, we consider the nonproduct observable $\mathcal{M}_{\det} = \sum_{i=1}^3 \sigma_i \otimes \sigma_i$ and $t = 3$. Note that even though the observable is nonproduct, the moments can still be obtained by local measurements, as the expectation value can be obtained from the three measurements $X \otimes X, Y \otimes Y, Z \otimes Z$ for a fixed choice of unitaries. The corresponding moment yields

$$\mathcal{R}_{\mathcal{M}_{\det}}^{(3)}(\rho) = \det(T) = I_1. \quad (9)$$

This scheme is not limited to bipartite systems. Indeed, it is possible to measure a mixed-state variant of the Kempe invariant of three-qubit systems [19,20]. We demonstrate this using the observable $\mathcal{M}_{\text{Kempe}} = Z \otimes Z \otimes 1 + Z \otimes 1 \otimes Z + 1 \otimes Z \otimes Z$ in Appendix A [21]. Before turning to the experimental implementation of the randomized measurement scheme, some statistical considerations are in order. For any fixed choice of local unitaries, multiple measurements are needed to obtain an estimate of the expectation value. Furthermore, a large number of random unitaries have to be chosen. We denote the number of random unitary choices by M , and the number of measurements per choice to obtain the expectation value by K ,

such that the total number of measurements is given by MK .

Central for this scheme is the generation of Haar random unitaries. We certify the randomness of unitaries in our setup by calculating their so-called frame potential as detailed in Appendix B [21].

Experimental methods.—We experimentally verify the functionality of the proposed randomized measurement method for the two-qubit case using polarization-entangled photon pairs. A schematic of our experimental setup is shown in Fig. 1(a). The entangled photon source (EPS) generates signal and idler photon pairs via four-wave mixing in a dispersion shifted fiber (DSF) [38]. The DSF is pumped with a 50 MHz pulsed fiber laser centered at 1552.52 nm and is arranged in a Sagnac loop with a polarizing beam splitter (PBS) to entangle the signal and idler in polarization. The photons are spectrally demultiplexed into 100 GHz-spaced channels on the International Telecommunication Union (ITU) grid after the Sagnac loop, resulting in photons with a temporal duration of about 15 ps [39,40]. For the experiment described here, ITU channels 27 (1555.75 nm) and 35 (1549.32 nm) are used. The source is tunable and typically outputs $\mu = 0.001$ – 0.1 pairs per pump pulse. Each photon is detected with gated InGaAs detectors with detection efficiencies of $\eta \sim 20\%$ and dark count probabilities of $\sim 4 \times 10^{-5}$ per gate [41,42].

Given the polarization-entangled state generated by our source, we must implement random local unitary rotations in the form of random polarization state rotations. Therefore, we utilize the scrambling function of automated polarization controllers in order to apply random

polarization rotations (for the remainder of the Letter, a polarization controller operating in scrambling mode will be referred to as a polarization scrambler).

After verifying that the polarization scramblers can be used to apply sufficiently random unitaries, we measured unbiased estimators (see Appendix C [21]) for the I_1 , I_2 , and I_3 invariants via Eqs. (7)–(9). Each polarization scrambler was set to rotate incident light to a random polarization state (therefore, acting as a random unitary), and coincidences were measured in different bases. To that end, we define for each of the two parties $i = 1, 2$ the local bases $\{|H\rangle_i, |V\rangle_i\}$ of horizontally and vertically polarized light, $\{|D\rangle_i, |A\rangle_i\}$ of diagonal and antidiagonal polarized light and $\{|L\rangle_i, |R\rangle_i\}$ of left circular and right circular polarized light. Note that while we associate these bases with polarization states, the unitary invariance of the measured quantities allows us to choose any local bases, as long as they are rotated by $(\pi/2)$ on the Bloch sphere with respect to each other. In particular, the bases for measuring photons 1 and 2 do not need to be aligned, i.e., $|H\rangle_1$ and $|H\rangle_2$ do not need to be equivalent on their respective Bloch spheres. We then measured in each combination of these local bases repeatedly for $M = 200$ different settings of the polarization scramblers, i.e., 200 different random unitaries were applied, where for each of these settings, $K \approx 1500$ repetitions were used to measure the expectation value.

The method to estimate I_1 , I_2 , and I_3 from finite measurement results is discussed in detail in Appendix C [21]. Although we collect measurement results in the $\{|H\rangle_i, |V\rangle_i\}$, $\{|D\rangle_i, |A\rangle_i\}$ and $\{|L\rangle_i, |R\rangle_i\}$ bases described above, the estimators for I_2 and I_3 only require projective measurements in a single joint basis. Therefore, those estimators are calculated using only a subset of the data, for example, the results for $|H\rangle_1|H\rangle_2$, $|H\rangle_1|V\rangle_2$, $|V\rangle_1|H\rangle_2$, and $|V\rangle_1|V\rangle_2$. On the other hand, the estimator for I_1 requires projective measurements in all three of the measured joint bases. After calculating the invariants, the experiment described above was repeated 25 different times to allow for a statistical analysis of the results.

The experimentally determined estimators of the I_1 , I_2 , and I_3 invariants for all 25 runs (each run is shown in a different color) are shown in Figs. 1(b)–1(d), respectively. The green band in all plots corresponds to the expected value of each invariant to allow for comparison with our method. The band represents the mean value plus or minus the standard deviation of each invariant calculated by performing quantum state tomography many times to characterize the state output by the EPS. A more-detailed description of how these expected values are calculated is found in Appendix E3 in the Supplemental Material [21]. The experimentally determined invariants converge near the expected values, therefore validating our randomized measurement protocol.

Applications to the detection of Bell nonlocality and teleportation fidelity.—The most straightforward application is the evaluation of $I_2 = \text{Tr}(TT^T)$, also known as the

two-body sector length [43]. A quantum state is entangled if $I_2 > 1$, and the maximal value is $I_2 = 3$ for Bell states. Note that additional knowledge of $I_3 = \text{Tr}(TT^T TT^T)$ allows for the detection of many more entangled states [12].

Combined knowledge of $I_1 = \det(T)$, $I_2 = \text{Tr}(TT^T)$, and $I_3 = \text{Tr}(TT^T TT^T)$ is useful for completely determining if a state’s nonlocality can be detected by a CHSH-like inequality: Given the observable [44]

$$\mathcal{B} = \sum_{i,j=1}^3 [a_i(c_j + d_j) + b_i(c_j - d_j)]\sigma_i \otimes \sigma_j, \quad (10)$$

where \vec{a} , \vec{b} , \vec{c} , and \vec{d} are real, normalized vectors, its expectation value is bounded by 2 for local states. For a given quantum state, the maximum expectation value that one can observe by varying the vectors that define the observable is given by $2\sqrt{\lambda_1^2 + \lambda_2^2}$, where λ_1 and λ_2 are the two largest singular values of the correlation matrix T [45]. Thus, the quantity

$$\text{CHSH}(\rho) = 2\sqrt{\lambda_1^2 + \lambda_2^2} - 2 \quad (11)$$

measures the observable violation.

As the squares of the singular values of T coincide with the eigenvalues of TT^T , we can obtain them by measuring the coefficients of the characteristic polynomial

$$p_T(x) = x^3 - \text{Tr}(TT^T)x^2 - \frac{1}{2}[\text{Tr}(TT^T TT^T) - \text{Tr}(TT^T)^2]x - \det(T)^2, \quad (12)$$

which are LU invariants, and calculating its roots. However, some care is needed to properly transfer statistical errors from finite statistics of the invariants to the roots of this polynomial; we explain the data analysis methods in Appendix D [21].

As a second figure of merit, we can decide whether a given two-qubit state is useful in a teleportation protocol. There, the maximal fidelity f_{\max} of the teleported state is given by [46]

$$f_{\max} = \frac{F_{\max}d + 1}{d + 1}, \quad (13)$$

where in our case $d = 2$ and F_{\max} is the maximal overlap of the distributed state with the maximally entangled state $|\phi^+\rangle = (1/\sqrt{2})(|00\rangle + |11\rangle)$ under local operations and classical communication. As local unitary rotations constitute a subset of these, we can lower bound F_{\max} by optimizing over LUs instead, yielding [47]

$$F_{\max} \geq F_{\max}^U := \frac{1}{4} \max\{1 - \lambda_1 - \lambda_2 - \lambda_3, 1 - \lambda_1 + \lambda_2 + \lambda_3, 1 + \lambda_1 - \lambda_2 + \lambda_3, 1 + \lambda_1 + \lambda_2 - \lambda_3\}. \quad (14)$$

By examining the invariants I_1 , I_2 and I_3 , we can minimize F_{\max}^U over all singular values λ_i which are compatible with the observed data, giving a lower bound on the teleportation fidelity of the prepared quantum state.

Results.—Using the methods described above and under the assumption that 25 repetitions of the experiment yields results which are well described by the Gaussian approximation, we extract the following experimental values for the invariants:

$$\det(T) = -0.62 \pm 0.15, \quad (15)$$

$$\text{Tr}(TT^T) = 2.41 \pm 0.15, \quad (16)$$

$$\text{Tr}(TT^T TT^T) = 2.21 \pm 0.21, \quad (17)$$

where the confidence regions correspond to 3σ , i.e., 99.73% confidence levels. These values are all in agreement with the values determined from quantum state tomography [shown by the green bands in Figs. 1(b)–1(d)]: $I_1 = -0.71 \pm 0.12$, $I_2 = 2.41 \pm 0.34$, and $I_3 = 1.95 \pm 0.34$ with 1σ confidence regions.

From these values, we obtain a potential CHSH violation of

$$\text{CHSH}(\rho) \geq 0.46. \quad (18)$$

The confidence of this violation is given by $0.991 \approx 2.6\sigma$, as detailed in Appendix D [21]. For comparison, the *maximal* CHSH violation calculated from quantum state tomography is $\text{CHSH}_{\text{QST}} \leq 0.60 \pm 0.11$. Note that the maximal observable value for a fully entangled state is given by $2\sqrt{2} - 2 \approx 0.83$.

Similarly, by requiring a higher confidence level of 5σ for the invariants, $\text{CHSH}(\rho) = 0.42$ with confidence $0.999998 \approx 4.7\sigma$ can be obtained.

Using either method, our results clearly show that the randomized measurement protocol successfully determines that the state output by our EPS has the potential to violate a CHSH inequality.

For the teleportation fidelity, a confidence level of 3σ of the LU invariants yields a fidelity of at least

$$F_{\max}^U = 0.88, \quad (19)$$

or, via Eq. (13), $f_{\max} = 0.92$, with a confidence level of $0.991 \approx 2.6\sigma$. By raising the confidence of the invariants to 5σ , the lower bound decreases to $F_{\max}^U = 0.86$, or $f_{\max} = 0.90$, with confidence $0.999998 \approx 4.7\sigma$. For comparison, the fidelity of the state calculated from tomography is $F_{\text{QST}} = 0.90 \pm 0.08$, and the teleportation fidelity is

$f_{\text{QST}} = 0.93 \pm 0.05$, confirming that the randomized measurement protocol accurately determines these parameters.

A detailed derivation of these values can be found in Appendix E, where we also give values for these quantities without the assumption of Gaussian distribution, by using the Hoeffding inequality instead [21].

Conclusion.—We showed that any local unitary invariant characterizing the quantum correlations in quantum states of two or more particles can be directly measured using the moments of randomized measurements. We exemplified this for two-qubit states, where we showed how all relevant LU invariants can be inferred from randomized measurements of appropriately chosen observables. We proceeded to demonstrate the practicality of the introduced methods by conducting an experiment with entangled photon pairs leading to an efficient measurement of the LU invariants I_1 , I_2 , and I_3 . The latter allowed us to directly certify important properties of the state, i.e., its Bell nonlocality as well as its usefulness for quantum teleportation. Furthermore, as a necessary by-product of our investigations, we devised methods allowing for a characterization of the degree of randomness of a set of experimentally implemented unitary transformations.

We emphasize the simplicity of the presented scheme which allows to infer several important properties of the underlying quantum state through a number of randomly assorted measurements. For this reason, it will be an interesting direction of future research to extend the present explicit constructions for two-qubit states also to higher-dimensional systems which likely will find ample applications in quantum communication tasks. Also, it would be desirable to extend our approach to the characterization of nonlocal quantum channels and multiparticle quantum correlations such as multi-setting Bell nonlocality or spin squeezing.

N. W. acknowledges support by the QuantERA project QuICHE via the German Ministry of Education and Research (BMBF Grant No. 16KIS1119K). A. K. acknowledges funding from the Ministry of Economic Affairs, Labour and Tourism Baden-Württemberg, under the project QORA. S. I. acknowledges support by the DAAD. J. L. B. acknowledges support from the House of Young Talents of the University of Siegen. O. G. acknowledges support by the Deutsche Forschungsgemeinschaft (DFG, German Research Foundation, Projects No. 447948357 and No. 440958198), the Sino-German Center for Research Promotion (Project No. M-0294), the ERC (Consolidator Grant No. 683107/TempoQ) and the German Ministry of Education and Research (Project QuKuK, BMBF Grant No. 16KIS1618K).

[1] M. C. Tran, B. Dakić, F. Arnault, W. Laskowski, and T. Paterek, *Phys. Rev. A* **92**, 050301(R) (2015).

- [2] L. Knips, J. Dziewior, W. Kłobus, W. Laskowski, T. Paterek, P. J. Shadbolt, H. Weinfurter, and J. D. A. Meinecke, *npj Quantum Inf.* **6**, 51 (2020).
- [3] L. Knips, *Quantum Views* **4**, 47 (2020).
- [4] A. Elben, S. T. Flammia, H.-Y. Huang, R. Kueng, J. Preskill, B. Vermersch, and P. Zoller, *Nat. Rev. Phys.* **5**, 9 (2023).
- [5] P. Cieřliński, S. Imai, J. Dziewior, O. Gühne, L. Knips, W. Laskowski, J. Meinecke, T. Paterek, and T. Vértesi, [arXiv:2307.01251](https://arxiv.org/abs/2307.01251).
- [6] D. Gross, K. Audenaert, and J. Eisert, *J. Math. Phys. (N.Y.)* **48**, 052104 (2007).
- [7] A. Ketterer, N. Wyderka, and O. Gühne, *Quantum* **4**, 325 (2020).
- [8] H.-Y. Huang, R. Kueng, and J. Preskill, *Nat. Phys.* **16**, 1050 (2020).
- [9] T. Brydges, A. Elben, P. Jurcevic, B. Vermersch, C. Maier, B. P. Lanyon, P. Zoller, R. Blatt, and C. F. Roos, *Science* **364**, 260 (2019).
- [10] A. Elben, R. Kueng, H.-Y. R. Huang, R. van Bijnen, C. Kokail, M. Dalmonte, P. Calabrese, B. Kraus, J. Preskill, P. Zoller, and B. Vermersch, *Phys. Rev. Lett.* **125**, 200501 (2020).
- [11] A. Ketterer, N. Wyderka, and O. Gühne, *Phys. Rev. Lett.* **122**, 120505 (2019).
- [12] S. Imai, N. Wyderka, A. Ketterer, and O. Gühne, *Phys. Rev. Lett.* **126**, 150501 (2021).
- [13] S. T. Flammia and Y.-K. Liu, *Phys. Rev. Lett.* **106**, 230501 (2011).
- [14] A. Elben, B. Vermersch, R. van Bijnen, C. Kokail, T. Brydges, C. Maier, M. K. Joshi, R. Blatt, C. F. Roos, and P. Zoller, *Phys. Rev. Lett.* **124**, 010504 (2020).
- [15] M. Grassl, M. Rötteler, and T. Beth, *Phys. Rev. A* **58**, 1833 (1998).
- [16] T. A. Springer, *Invariant Theory* (Springer, New York, 2006), Vol. 585.
- [17] Y. Makhlin, *Quantum Inf. Process.* **1**, 243 (2002).
- [18] B.-Z. Sun, S.-M. Fei, and Z.-X. Wang, *Sci. Rep.* **7**, 4869 (2017).
- [19] J. Kempe, *Phys. Rev. A* **60**, 910 (1999).
- [20] H. Barnum and N. Linden, *J. Phys. A* **34**, 6787 (2001).
- [21] See Supplemental Material at <http://link.aps.org/supplemental/10.1103/PhysRevLett.131.090201> for the appendices, which include Refs. [22–35].
- [22] A. Sanpera, R. Tarrach, and G. Vidal, *Phys. Rev. A* **58**, 826 (1998).
- [23] K. Bartkiewicz, J. Beran, K. Lemr, M. Norek, and A. Miranowicz, *Phys. Rev. A* **91**, 022323 (2015).
- [24] R. Augusiak, M. Demianowicz, and P. Horodecki, *Phys. Rev. A* **77**, 030301(R) (2008).
- [25] K. Bartkiewicz, P. Horodecki, K. Lemr, A. Miranowicz, and K. Życzkowski, *Phys. Rev. A* **91**, 032315 (2015).
- [26] A. J. Scott, *J. Phys. A* **41**, 055308 (2008).
- [27] N. Hunter-Jones, [arXiv:1905.12053](https://arxiv.org/abs/1905.12053).
- [28] I. M. Gessel, *J. Comb. Theory Ser. A* **53**, 257 (1990).
- [29] B. Ghosh, *Am. Stat.* **56**, 186 (2002).
- [30] J. M. Renes, *Frames, Designs, and Spherical Codes in Quantum Information Theory* (The University of New Mexico, Albuquerque, 2004).
- [31] J. Newcomer, Estimation procedures for multinomial models with overdispersion, Ph.D. Thesis, University of Maryland, Baltimore County, 2008.
- [32] W. Hoeffding, in *The Collected Works of Wassily Hoeffding* (Springer, New York, 1994), pp. 409–426.
- [33] D. E. Jones, B. T. Kirby, and M. Brodsky, *npj Quantum Inf.* **4**, 58 (2018).
- [34] B. T. Kirby, D. E. Jones, and M. Brodsky, *J. Light. Technol.* **37**, 95 (2018).
- [35] D. E. Jones, B. T. Kirby, G. Riccardi, C. Antonelli, and M. Brodsky, *New J. Phys.* **22**, 073037 (2020).
- [36] G. Vidal and R. F. Werner, *Phys. Rev. A* **65**, 032314 (2002).
- [37] B. Collins, S. Matsumoto, and J. Novak, *Not. Am. Math. Soc.* **69** (2022).
- [38] M. Fiorentino, P. L. Voss, J. E. Sharping, and P. Kumar, *IEEE Photonics Technol. Lett.* **14**, 983 (2002).
- [39] S. X. Wang and G. S. Kanter, *IEEE J. Sel. Top. Quantum Electron.* **15**, 1733 (2009).
- [40] NuCrypt, Quantum optical instrumentation, <http://nucrypt.net/quantum-optical-instrumentation.html>, accessed: 2022-10-11.
- [41] D. E. Jones, B. T. Kirby, and M. Brodsky, in *Frontiers in Opt.* (Optical Society of America, 2017), pp. JW4A–37, [10.1364/FIO.2017.JW4A.37](https://doi.org/10.1364/FIO.2017.JW4A.37).
- [42] D. E. Jones, B. T. Kirby, and M. Brodsky, in *IEEE Photonics Society Summer Topical Meeting Series* (IEEE, New York, 2017), pp. 123–124, [10.1109/PHOSST.2017.8012681](https://doi.org/10.1109/PHOSST.2017.8012681).
- [43] N. Wyderka and O. Gühne, *J. Phys. A* **53**, 345302 (2020).
- [44] F. Verstraete and M. M. Wolf, *Phys. Rev. Lett.* **89**, 170401 (2002).
- [45] R. Horodecki, P. Horodecki, and M. Horodecki, *Phys. Lett. A* **200**, 340 (1995).
- [46] M. Horodecki, P. Horodecki, and R. Horodecki, *Phys. Rev. A* **60**, 1888 (1999).
- [47] O. Gühne, Y. Mao, and X.-D. Yu, *Phys. Rev. Lett.* **126**, 140503 (2021).